

Modeling and Optimization Study of a Regenerative Cooling Channel with Endothermic Reaction of Hydrocarbon Aviation Fuels

Seung Hyeon Lee* and Hyung Ju Lee*†

* Department of Mechanical Engineering, Pukyong National University
45 Yongso-ro, Nam-gu, Busan 48513, Republic of Korea
anminster@pukyong.ac.kr – hj.lee@pknu.ac.kr

† Corresponding Author

Abstract

A one-dimensional simulation code was developed to analyze regenerative cooling in a microchannel, where liquid hydrocarbon fuels undergo endothermic decomposition. To quantitatively assess fuel states under varying heat flux–mass flow rate conditions, a working state map and heat sink ratio (τ_h) were applied. The states were classified as subcritical, supercritical, thermal cracking, and risking, based on the thermal limit of the metal (1000 K) and the corresponding fuel behavior. Channels with smaller width, height, and fin thickness but larger wall thickness enabled broader operability. Under identical conditions, n-dodecane was evaluated to have a wider operational range than n-decane.

Nomenclature

| | |
|-------------|--|
| A | Pre-exponential factor in Arrhenius equation (1/s) |
| A_f | Effective heat transfer area of wall (m ²) |
| A_t | Total wetted area of wall surface exposed to coolant (m ²) |
| A_{CS} | Cross-sectional area of wall (m ²) |
| C_p | Specific heat at constant pressure (J/(kg·K)) |
| d | Hydraulic diameter of cooling channel (m) |
| E_a | Activation energy (J/mol) |
| f | Darcy friction factor |
| h | Specific enthalpy of fluid (J/kg) |
| H | Channel height (m) |
| k | Reaction rate (1/s) |
| Nu | Nusselt number |
| P | Pressure (Pa) |
| Pr | Prandtl number |
| q_f | Heat flux from wall to coolant (W/m ²) |
| Q_w | Net heat transfer across wall (W) |
| R | Universal gas constant (J/(mol·K)) |
| Re | Reynolds number |
| T_f | Bulk fluid temperature (K) |
| t_f | Fin thickness (m) |
| T_w | Wall temperature (K) |
| t_w | Wall thickness (m) |
| u | Axial velocity (m/s) |
| W | Channel width (m) |
| x | Axial position (m) |
| Y | Mass fraction of thermal cracking reactant |
| α | Heat transfer coefficient (W/(m ² ·K)) |
| δ | Absolute roughness of channel wall (m) |
| η_t | Overall fin efficiency |
| λ | Thermal conductivity of fluid (W/(m·K)) |
| λ_w | Thermal conductivity of wall material (W/(m·K)) |
| μ | Dynamic viscosity of fluid (Pa·s) |
| μ_f | Viscosity at fluid temperature (Pa·s) |
| μ_w | Viscosity at wall temperature (Pa·s) |

ρ Density of fluid (kg/m³)

1. Introduction

Regenerative cooling is one of the representative thermal management strategies designed to protect the airframe and scramjet combustor of hypersonic vehicles from high-temperature heating effects [1]. Typically, liquid hydrocarbon fuel flows through the regenerative cooling channels, where it not only lowers the wall temperature effectively through convective heat transfer and endothermic decomposition, but also gains the advantage of enhanced combustion efficiency due to improved mixing and combustion stability under the short residence time in the supersonic combustor [2]. In such a regenerative cooling system, the cooling performance is determined by the fuel's flow, heat transfer, and chemical reaction characteristics, which are strongly influenced by channel geometry and operating conditions such as system pressure, mass flow rate, and surface heat flux. Numerical simulations are commonly employed to analyze the complex interactions occurring inside the channels; however, multidimensional simulations capable of accurate modeling require significant computational cost. Therefore, for the efficient design of regenerative cooling systems, it is essential to develop a one-dimensional performance analysis code that allows for the exploration of optimal combinations of channel geometry and operating conditions at a relatively low cost, as well as the implementation of fuel control strategies.

Based on this background, previous studies have proposed one-dimensional heat transfer analysis models to effectively predict the regenerative cooling performance of hypersonic vehicles [3,4], and some of them have incorporated pyrolysis reactions to derive fuel operation strategies according to flight conditions [4]. However, most existing studies have been limited to specific geometries or operating conditions, and few researchers have addressed the systematic classification of fuel states and their stability under various configurations and conditions.

Therefore, in this study, a one-dimensional simulation code was developed to analyze regenerative cooling in a microchannel, where liquid hydrocarbon fuels undergo endothermic decomposition. To enable visual classification of fuel states and wall temperature behavior under varying heat flux–mass flow rate combinations, a working state map was introduced [5]. In particular, the operational regime in this map was divided into subcritical, supercritical, thermal cracking, and risking zones, and the heat sink ratio (r_h), an index representing the relative proportion between chemical and physical heat sinks, was applied [6]. Based on the analysis results, the maximum r_h line, which represents the maximum chemical heat sink releasing rate for various fuels and channel geometries, was additionally presented on the working state map.

2. Numerical methodology

2.1 Channel configuration and modeling assumptions

Although the regenerative cooling system of an actual hypersonic vehicle consists of a complex structure with multiple parallel channels, a single cooling channel with a rectangular cross-section, as shown in Figure 1, was selected as the target of this study to simplify the model. The geometric design variables of the cooling channel include the thickness of the heated wall (t_w), the thickness of the fin (t_f), the width (W), the height (H), and the axial length (L). In this analysis, the axial length was fixed at 1 m. To further simplify the analysis, the following major assumptions were applied:

- (1) The flow inside the cooling channel is assumed to be one-dimensional and steady, with a constant cross-sectional area along the axial direction.
- (2) The heat flux applied to the wall is uniform, and all the heat is absorbed by the fuel.
- (3) Gravitational effects are neglected, and conjugated heat transfer with the combustor is excluded from the scope of this analysis.

2.2 Thermophysical property prediction methods

In this analysis, n-decane (C₁₀H₂₂) and n-dodecane (C₁₂H₂₆), which are the main components of JP-7 and JP-8 aviation fuels, were used as the fuels for the cooling channel. To account for property variations in the supercritical regime, the following prediction methods were applied for each thermophysical property. The density and constant pressure specific heat (C_p) were calculated using the RK-PR EoS (Redlich-Kwong-Peng-Robinson Equation of State) [7], while the viscosity was estimated based on the correlation proposed by Chung et al. [8,9], and the thermal conductivity was calculated using the modified propane-based TRAPP (TRANsport Property Prediction) method [10,11]. The predicted properties of n-decane and n-dodecane under 3 MPa were compared with NIST data, and both fuels showed reasonably

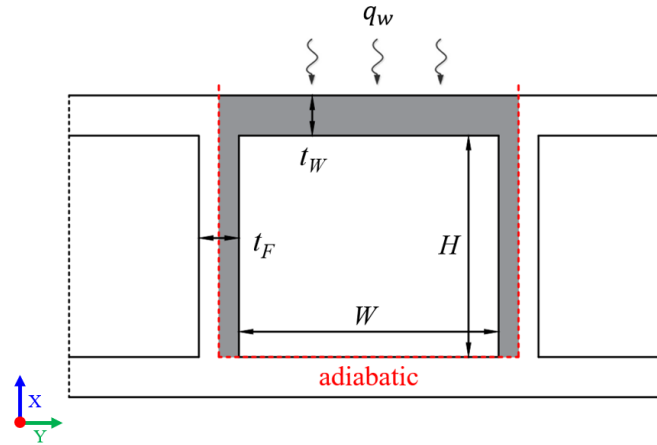


Figure 1: Schematic of the simplified rectangular unit channel model for numerical analysis

good agreement in terms of property variation trends in both subcritical and supercritical regimes. In addition, the same property prediction methods were applied to the major product species generated through pyrolysis reactions. The thermophysical properties of the resulting mixtures were computed using a mixing rule based on the mass fractions of individual species, which was identical to that used in a previous study [12].

2.3 One-dimensional modeling

To facilitate the analysis, the computational domain of the regenerative cooling channel was divided into a fluid domain and a solid domain, as shown in Figure 2. The governing physical phenomena in each region were treated separately, and the corresponding formulations were established. The governing equations for the fluid domain are presented in Section 2.3.1, while the heat transfer equations for the solid domain are provided in Section 2.3.2.

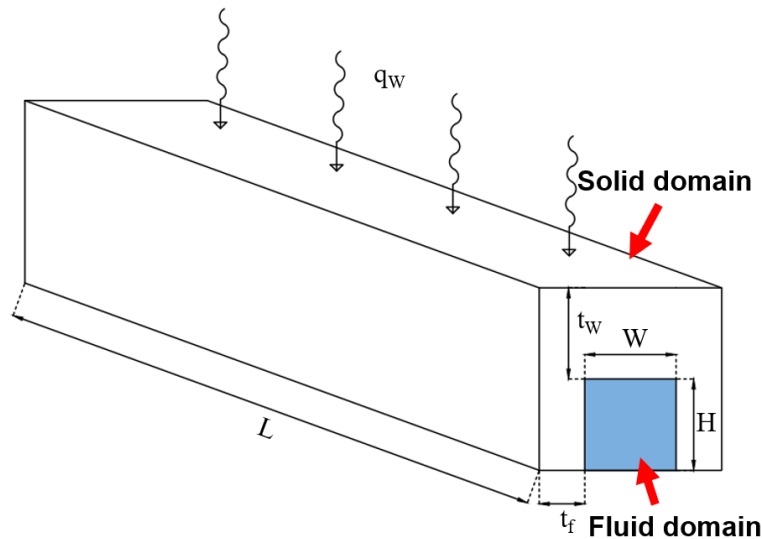


Figure 2: Schematic diagram of the regenerative cooling channel with designated solid and fluid domains

2.3.1 Modeling on the fluid domain

The numerical analysis of the internal flow in the regenerative cooling channel was performed based on the following conservation equations of mass, momentum, energy, and species in the fluid domain:

$$\frac{\partial(\rho u)}{\partial x} = 0 \quad (1)$$

$$\frac{\partial P}{\partial x} = -\frac{1}{2} \frac{f \rho u^2}{d} \quad (2)$$

$$\frac{\partial(\rho u h)}{\partial x} = \frac{4}{d} q_f \quad (3)$$

$$\frac{\partial(\rho u Y)}{\partial x} = \rho Y k \quad (4)$$

Here, the friction factor f and wall heat flux q_f are defined as follows:

$$f = \begin{cases} \frac{64}{Re} & , Re \leq 2320 \\ 0.11 \left(\frac{\delta}{d} + \frac{68}{Re} \right)^{-0.25} & , Re > 2320 \end{cases} \quad (5)$$

$$q_f = \alpha(T_w - T_f) = \frac{\lambda}{d} Nu(T_w - T_f) \quad (6)$$

Depending on the bulk temperature T_f of the fuel, different Nusselt number correlations are applied as follows [3]:

$$Nu = \begin{cases} 0.027 Re^{0.8} Pr^{0.333} \left(\frac{\mu_f}{\mu_w} \right)^{0.14} & , T_f \leq 800 K \\ 0.024 Re^{0.83} Pr^{0.4} \left(\frac{\mu_f}{\mu_w} \right)^{0.1} & , T_f > 800 K \end{cases} \quad (7)$$

The Reynolds number and Prandtl number are defined as:

$$Re = \frac{\rho u d}{\mu}, \quad Pr = \frac{c_p \mu}{\lambda} \quad (8)$$

2.3.2 Modeling on the solid domain

Heat transfer in the wall was modeled by considering both the convective heat transfer between the wall and the fuel, and the axial conduction within the wall, as expressed by the following equation:

$$Q_w = q_f A_f - \lambda_w A_{cs} \frac{\partial^2 T_w}{\partial x^2} \quad (9)$$

Assuming that the wall between channels (with thickness t_f) was treated as an adiabatic tip, the total heat transfer through the wall was calculated using the overall fin efficiency, as follows:

$$Q_w = q(t_f + W) \quad (10)$$

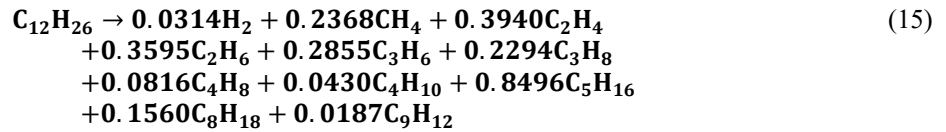
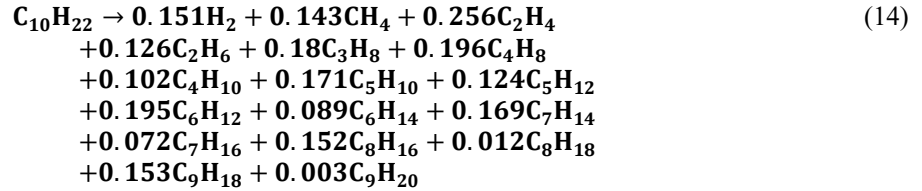
$$A_f = A_t \eta_t \quad (11)$$

$$A_t = 2(H - t_w) + W \quad (12)$$

$$\eta_t = \frac{\tanh\left((2\alpha/\lambda_w t_f)^{1/2}(H-t_w)+t_f/2\right)}{(2\alpha/\lambda_w t_f)^{1/2}(H-t_w)+t_f/2} \quad (13)$$

2.4 Pyrolysis model

For chemical reaction modeling, the global reaction PPD (Proportional Product Distribution) model was adopted. The pyrolysis product distribution for each fuel was constructed based on Refs. [13, 14], and the reaction equations for each are as follows:



The reaction rate for both fuels follows the Arrhenius equation and is expressed as follows:

$$k = A \cdot e^{-E_a/(RT_f)} \quad (16)$$

For n-decane, the pre-exponential factor and activation energy were $A = 2.44 \cdot 10^{14} \text{ s}^{-1}$, $E_a = 225.8 \text{ kJ/mol}$, respectively. For n-dodecane, $A = 1.6 \cdot 10^{15} \text{ s}^{-1}$, $E_a = 246.02 \text{ kJ/mol}$ were applied.

2.5 Solver configuration and grid setup

The simulation was carried out under steady-state conditions, employing an explicit forward Euler method with a first-order finite difference discretization scheme. The entire computational domain was divided into n grid nodes with uniform spacing along the channel length L . To evaluate the sensitivity of the solution to the number of grids, a grid independence test was conducted. By applying various numbers of grid points ranging from 10 to 100 for the total channel length, it was observed that the outlet temperature started to converge stably when the number of grids exceeded approximately 40, and the variation rate subsequently decreased to below 1%. Accordingly, considering both computational accuracy and cost, the total number of grids was set to 50 for all simulations in this study.

3. Results and discussion

3.1 Parametric cases and operating conditions

The geometric parameters of the rectangular cross-section channels used in this study are summarized in Table 1. In the baseline case (Case (a)), the channel width (W) and height (H) were set to 1 mm, the fin thickness (t_f) to 0.5 mm, the wall thickness (t_w) to 1 mm, and the channel length (L) was kept constant at 1 m. To analyze the influence of geometric variation on cooling channel performance, four additional cases were defined based on modifications from the baseline. In Case (b), the channel width was doubled. In Case (c), the channel height was doubled. Case (d) reduced the fin thickness by half, while Case (e) increased the wall thickness by a factor of two.

Meanwhile, the operating conditions used in the analysis are presented in Table 2. The outlet pressure was kept constant at 3 MPa, and the inlet temperature was set to 373.15 K. The inlet mass flow rate was varied from 0.5 g/s to 5 g/s, and the wall heat flux ranged from 5 kW/m² to 4,000 kW/m². These settings enabled systematic comparison and analysis of cooling performance under a variety of channel geometries and operating conditions.

3.2 Simulation results

Figure 3 shows a typical working state map for regenerative cooling systems using n-decane under the default channel geometry. By analyzing the operational region and key boundary lines (Transcritical line, Initial cracking line, Optimal

performance line, and Risking line) with respect to mass flow rate and heat flux for the five cases, it was observed that in most configurations, the Optimal performance line lies above the Risking line. Therefore, practical operation is generally limited to the thermal cracking zone, which lies between the Risking line and the Initial cracking line. As the heat sink performance improves near the Risking line, the structural risk also increases, requiring a balanced consideration between cooling performance and system stability.

Table 1: Parameters of rectangular channel geometries

| cross section shape | W (mm) | H (mm) | t_f (mm) | t_w (mm) | L (m) |
|------------------------|----------|----------|------------|------------|---------|
| (a) default | 1 | 1 | 0.5 | 1 | 1 |
| (b) 2x Width | 2 | 1 | 0.5 | 1 | 1 |
| (c) 2x Height | 1 | 2 | 0.5 | 1 | 1 |
| (d) 0.5x Fin thickness | 1 | 1 | 0.25 | 1 | 1 |
| (e) 2x Wall thickness | 1 | 1 | 0.5 | 2 | 1 |

Table 2: Operating conditions

| Parameter | Value |
|----------------------|-----------------------------|
| Outlet pressure | 3 MPa |
| Inlet temperature | 373.15 K |
| Inlet Mass flow rate | 0.5 ~ 5 g/s |
| Constant heat flux | 5 ~ 4,000 kW/m ² |

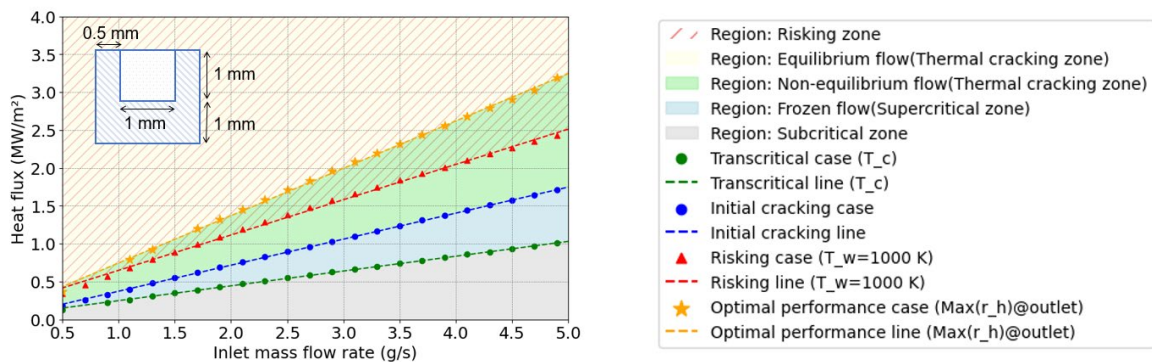


Figure 3: Working state maps for regenerative cooling channels with n-decane for the default channel configuration

The trends according to geometric variation are as follows. In the case of increased channel width (Case (b)) or height (Case (c)), the operational region becomes narrower due to decreased flow velocity and increased residence time caused by the enlarged cross-sectional area, indicating higher sensitivity to heat flux. On the other hand, reducing fin thickness (Case (d)) expands the operational range due to reduced heat input area and improved heat transfer efficiency of the fins. Increasing wall thickness (Case (e)) helps suppress wall temperature rise through increased thermal resistance, thereby slightly expanding the operational region, although structural concerns must also be considered. In addition, a comparison of the working state maps of n-decane and n-dodecane for the baseline geometry (Case (a)) has been made. It reveals that n-dodecane undergoes thermal cracking at a lower heat flux compared to n-decane, resulting in a broader thermal cracking zone. This trend originates from the fuel's property of initiating thermal decomposition at relatively lower temperatures. Consequently, n-dodecane is considered more viable than n-decane, as it allows for a wider range of operational heat flux.

4. Summary and Conclusions

In this study, a one-dimensional performance analysis model was developed for regenerative cooling microchannels used in hypersonic vehicles, with n-decane and n-dodecane as working fluids. The model integrates flow, heat transfer, and pyrolysis reactions. The working state map and heat sink ratio (r_h) were utilized to visualize the operable conditions, and it was confirmed that the maximum r_h condition corresponds to a dominant contribution of chemical heat sink, which enhances the endothermic effect but also increases structural risk due to higher wall temperature. From the analysis of geometric variations, it was observed that reducing the channel width, height, and fin thickness, and increasing the wall thickness, tends to expand the operable range under high heat flux conditions. However, as the channel cross-section becomes smaller, the risk of coke accumulation due to fuel pyrolysis increases. Moreover, increasing wall thickness may lead to thermal accumulation during long-term operation. Therefore, a geometry optimization strategy is required to ensure simultaneous performance improvement and structural reliability. In the comparison between fuels, n-dodecane tended to initiate pyrolysis at lower heat flux levels than n-decane, thereby expanding the operable region. The proposed model provides a useful framework for the design of regenerative cooling systems and the development of fuel control strategies, and it can be further extended toward design optimization through integration with experiments and multidimensional simulations in future studies.

Acknowledgement

This research was supported by the Basic Science Research Program through the National Research Foundation (NRF) of Korea, funded by the Ministry of Education (No. RS-2021-NR065835).

References

- [1] S. Luo, D. Xu, J. Song, and J. Liu. 2021. A review of regenerative cooling technologies for scramjets. *Applied Thermal Engineering* 190:116754.
- [2] H. J. Lee. 2020. Technical analysis of thermal decomposition characteristics of liquid hydrocarbon fuels for a regenerative cooling system of hypersonic vehicles. *Journal of Aerospace System Engineering* 14(4):32–39.
- [3] W. Bao, X. Li, J. Qin, W. Zhou, and D. Yu. 2012. Efficient utilization of heat sink of hydrocarbon fuel for regeneratively cooled scramjet. *Applied Thermal Engineering* 33–34:208–218.
- [4] D. Han, J. S. Kim, and K. H. Kim. 2022. Conjugate thermal analysis of X-51A-like aircraft with regenerative cooling channels. *Aerospace Science and Technology* 126:107614.
- [5] C. Zhang, H. Gao, J. Zhao, G. Yao, and D. Wen. 2023. Working state map of hydrocarbon fuels for regenerative cooling. *Propulsion and Power Research* 12(2):199–211.
- [6] Y. Feng, S. Zhang, J. Cao, J. Qin, Y. Cao, and H. Huang. 2016. Coupling relationship analysis between flow and pyrolysis reaction of endothermic hydrocarbon fuel in view of characteristic time correlation in mini-channel. *Applied Thermal Engineering* 102:661–671.
- [7] M. Cismondi, and J. Mollerup. 2005. Development and application of a three-parameter RK-PR equation of state. *Fluid Phase Equilibria* 232:74–89.
- [8] T. H. Chung, L. L. Lee, and K. E. Starling. 1984. Applications of kinetic gas theories and multiparameter correlation for prediction of dilute gas viscosity and thermal conductivity. *Industrial & Engineering Chemistry Fundamentals* 23(1):8–13.
- [9] T. H. Chung, M. Ajlan, L. L. Lee, and K. E. Starling. 1988. Generalized multiparameter correlation for nonpolar and polar fluid transport properties. *Industrial & Engineering Chemistry Research* 27(4):671–679.

- [10] B. E. Poling, J. M. Prausnitz, and J. P. O'Connell. 2001. *The Properties of Gases and Liquids*. 5th ed. McGraw-Hill Education Press, New York, USA.
- [11] J. Millat, J. H. Dymond, and C. A. Niero de Castro. 1996. *Transport Properties of Fluids: Their Correlation, Prediction and Estimation*. Cambridge University Press, Cambridge, UK.
- [12] J. Wang, H. Jin, H. Gao, and D. Wen. 2022. Cooling capacity optimization of hydrocarbon fuels for regenerative cooling. *Applied Thermal Engineering* 200:117661.
- [13] T. A. Ward, J. S. Ervin, R. C. Striebich, and S. Zabarnick. 2004. Simulations of flowing mildly-cracked normal alkanes incorporating proportional product distributions. *Journal of Propulsion and Power* 20(3):488–495.
- [14] D. Zhang, L. Hou, M. Gao, and X. Zhang. 2018. Experiment and modeling on thermal cracking of n-dodecane at supercritical pressure. *Energy & Fuels* 32(12):12455–12464.